JOURNAL OF GEOPHYSICAL RESEARCH, VOL. 112, D08213, doi:10.1029/2006JD007791, 2007

Click Here for Full Article

Sensitivity of the shortwave radiative budget to the parameterization of ice crystal effective radius

G.-J. van Zadelhoff,[1] E. van Meijgaard,[1] D. P. Donovan,[1] W. H. Knap,[1] and R. Boers[1]

Received 14 July 2006; revised 22 December 2006; accepted 10 January 2007; published 25 April 2007.

[1] A new effective particle size (R_{eff}) parameterization for ice clouds has been formulated based on depth into cloud relative to cloud top. This parameterization has been developed based on an extensive data set of lidar and radar ice cloud retrievals. Using this parameterization within the stand-alone radiation code from the European Centre for Medium Range Weather Forecasting (cy23r4), the performance of the new parameterization is compared with the more commonly used parameterizations based on temperature and/or ice water content. An evaluation is performed on the basis of observed shortwave fluxes for 13 days with persistent ice cloud decks, with no liquid clouds beneath, over the Cabauw Experimental Site for Atmospheric Research in the Netherlands. For each of these clouds the shortwave flux is calculated after which the distribution of the differences between the observed and modeled shortwave fluxes from the combined 13 days are compared with each other. The new parameterization shows a median absolute difference of 0.7 W m^{-2} relative to the observations. The control parameterization based on temperature shows a median absolute difference of 15 W m^{-2}. Within the framework of the KNMI regional climate model (RACMO2), the new parameterization yields an effective particle size versus temperature distribution very similar to the observed distributions from lidar and radar retrievals. Results from a 1-year integration indicate that the domain averaged monthly mean planetary albedo and transmissivity change by a maximum of 2.6 and 2.4%, respectively, using the new parameterization compared to the temperature-based parameterization.

Citation: van Zadelhoff, G.-J., E. van Meijgaard, D. P. Donovan, W. H. Knap, R. Boers (2007), Sensitivity of the shortwave radiative budget to the parameterization of ice crystal effective radius, *J. Geophys. Res.*, *112*, D08213, doi:10.1029/2006JD007791.

1. Introduction

[2] Ice clouds play an important role in the energy balance of the atmosphere. They can either cause cooling or warming depending on their altitude, ice water content (IWC), and microphysical properties like the particle effective radius(R_{eff}) and ice crystal habit. The latter is needed to account for the nonsphericity of ice crystals. The effective radius (here defined in terms of the mass and cross-sectional area of the particles) is intended to describe the effective size at which radiation interacts with individual particles. Describing R_{eff} properly is important as it directly affects the extinction of the solar radiation for a given IWC and hence the local shortwave (SW) transmissivity and reflectivity.

[3] Ice clouds are notoriously difficult to represent in climate models due to uncertainties in ice cloud properties and the inability to adequately account for the complex interactions between radiation, microphysics, and macrophysics within these clouds. The latter is primarily a resolution problem while the former is caused by the lack of coherent global observations; as a result of which, current parameterizations are based on measurements made during single campaigns or a combination of campaigns. Also, a lack of the understanding of ice cloud properties hampers progress. For example, in spite of the availability of measurements, great uncertainty still exists surrounding the concentrations of small ice crystals. Properties derived in this way could be biased due to local or temporal conditions and may not be valid for the full region used in the climate model. In several articles the sensitivity of the radiative fluxes to the assumed R_{eff} parameterizations has been examined [e.g., *Petch*, 1998; *Iacobellis et al.*, 2003; *McFarquhar et al.*, 2003], approaching the same problem from different sides. In the paper by Petch, the R_{eff} sensitivity of the SW flux within the model is tested. The latter two papers mentioned look at the SW flux sensitivity due to changes in the R_{eff} parameterizations by simulating profiles over remote sensing sites. In the present work the sensitivity of the model is only examined for changes in the radiation code. The atmospheric column is based on observations from a ground-based remote sensing site and not on a model prediction.

[4] A new parameterization for R_{eff}, adopting *Francis et al.*'s [1994] definition of R_{eff} (R_{eff} = [3 IWC]/[$4\rho_i A_c$], where ρ_i is the density of ice and A_c is the cumulative cross-sectional area of all ice particles; see the work of

[1]Royal Netherlands Meteorological Institute, De Bilt, The Netherlands.

Copyright 2007 by the American Geophysical Union.
0148-0227/07/2006JD007791$09.00

McFarquhar and Heymsfield [1998] for a detailed discussion on R_{eff} definitions), was described in the work of *van Zadelhoff et al.* [2004, G.-J. van Zadelhoff et al., An effective radius parameterization for ice clouds using cloud thickness, submitted to *Geophysical Research Letters*, 2007]. It is derived from the 2 years of observations obtained at two climatologically different sites. Its formulation is based on depth into cloud from cloud top in contrast to more commonly used parameterizations based on temperature, ice water content (IWC), or adopting fixed sizes. The parameterization results in an effective particle size versus temperature distribution very similar to the observed distributions at both sites. This is in contrast to the other parameterizations that do retrieve a reasonable mean $R_{\text{eff}}(T)$ but yield different R_{eff} distributions at different sites.

[5] The apparent strong relationship between depth into cloud and R_{eff} is linked to a simple conceptual model of cirrus cloud processes. Near the cloud top in nucleation regions, cloud particles will tend to be small. After formation these particles fall through the cloud and increase in size due to vapor deposition and aggregation [*Mitchell et al.*, 1996] until sublimation becomes dominant, resulting in smaller particles lower in the cloud.

[6] Temperature has been shown to have an important effect on both the ice habit formation [*Bailey and Hallett*, 2000] and the particle size distribution [*Mitchell*, 1994], for example, the difference in saturation vapor pressure between water and ice is directly related to temperature and, consequently, to the ice crystal growth rate. Temperature therefore has an influence on the R_{eff} but it appears not to be the main cause for the apparent $R_{\text{eff}}(T)$ relationship at these two sites. The observation that $R_{\text{eff}}(T)$ and $R_{\text{eff}}(\text{IWC},T)$ relationships are different for the CloudNET and Atmospheric Radiation Measurement Program Southern Great Plains (ARM-SGP) sites while a single parameterization based on cloud thickness works for both sites indicates that the R_{eff} may be relatively more influenced by the particles position in its life-cycle (which is related to its normalized depth into the cloud) and not by the immediate conditions they find themselves in.

[7] It is conceivable that climate models using a $R_{\text{eff}}(\text{IWC},T)$ parameterizations undergo an unrealistic extra forcing due to the temperature-based parameterization when the temperature alters because of climate change. Even when this extra forcing due to the temperature-dependent optical properties is small in size, its sign is persistent, and its effects may accumulate in the long run. Parameterizations based on cloud depth would not be directly affected by tropospheric temperature changes.

[8] In this paper we utilize the regional climate model RACMO2 [*Lenderink et al.*, 2003; *de Bruyn and van Meijgaard*, 2005] which was developed at KNMI in recent years by porting the physics package of the European Centre for Medium Range Weather Forecasting (ECMWF) Integrated Forecast System (IFS), release cy23r4, into the prognostic component of the hydrostatic HIRLAM NWP, version 5.0.6 [*Undén*, 2002]. The ECMWF physics package [*White*, 2002] of this cycle also served as the basis for the ERA40 project. Of relevance to this paper is the shortwave radiation module, which was originally developed by *Fouquart and Bonnel* [1980]. The current version solves the radiation transfer equation in four spectral bands, one in the ultraviolet and visible band (0.21–0.69 μm) and three in the near-infrared region (0.69–1.19, 1.19–2.38, 2.38–4.00 μm). Upward and downward fluxes are obtained from the reflectance and transmittance of the model layers, and the photon-path-distribution method is used to separate the scattering from the molecular absorption. The treatment of the interaction of solar radiation with ice clouds will be described hereafter.

[9] Within a climate model like RACMO2 the three model parameters that are linked when calculating the radiative effects of ice clouds are the R_{eff}, the IWC, and the cloud fraction. Because of the feedbacks between the three parameters, changes to only one of these parameters will result in changes in the radiative heating within the model but are not expected to yield a direct improvement of the model. In order to achieve this, the representation of all three parameters has to be improved simultaneously. The present work is the first step toward this goal; we test how the model responds to different R_{eff} parameterizations and use observationally derived IWC and cloud-fractions to compare the radiative transfer calculations to observed surface shortwave fluxes (global irradiances).

[10] The organization of this paper is as follows. In section 2 the parameterizations of R_{eff} are described. These are used in section 3 to calculate the radiative transfer in a single column for which the atmosphere is defined. In section 4 the results are statistically compared for 13 days of observations. Section 5 describes how the new R_{eff} parameterization is implemented in the regional climate model. Section 6 discusses the main differences for the entire RACMO2 grid as calculated for the different parameterizations. Finally, our conclusions are presented in section 7.

2. Effective Radius Parameterizations for Use in Climate Models

[11] In this work, four different parameterizations of R_{eff} are compared. All are diagnostic, with R_{eff} based on (1) temperature, (2) IWC and temperature, (3) adopting a constant value for R_{eff}, and (4) using geometrical cloud thickness. The first one under consideration is the current RACMO2 parameterization adopted from a former version of the ECMWF-IFS (cy23r4). This parameterization (a revision from the work of *Ou and Liou* [1995]), hereafter referred to as $R_{\text{eff}}(T)$, is based on temperature only, with a linear transition in R_{eff} from 30 to 60 μm between -60° and -40°C. The values are assumed to be constant outside this temperature regime (30 μm for $T < -60^\circ$C and 60 μm for $T > -40^\circ$C). The second parameterization is part of a very recent version of the ECMWF-IFS (cy30r1). It uses a combination of IWC and temperature, based on the work by *Sun and Rikus* [1999] and *Sun* [2001], hereafter referred to as the $R_{\text{eff}}(\text{IWC},T)$ parameterization. This parameterization links the optical thickness to IWC and temperature only. Both parameterizations are chosen since they are part of the ECMWF radiation scheme and are and have therefore been used extensively (for example, ERA-40 ($R_{\text{eff}}(T)$)). Even though the $R_{\text{eff}}(\text{IWC},T)$ parameterization in question has been criticized in the literature [*McFarquhar*, 2001] because of the simplified assumption of a single ice crystal habit (hexagonal columns) making it inconsistent with the

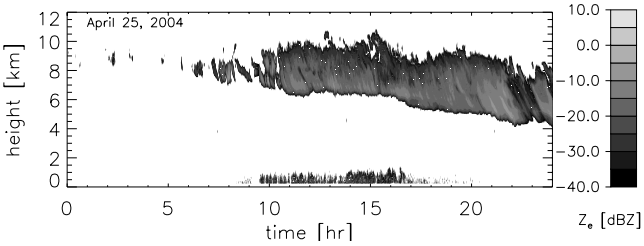

Figure 1. Measured radar reflectivity (dBZ) of a persistent ice cloud at Cabauw for 25 April 2004. The daytime reflectivity below 1.5 km is primarily caused by insects and aerosol.

observed mass and area contents, it has continued to remain part of the ECMWF-IFS, and it is therefore used in the comparison presented here. The abbreviations of $R_{\text{eff}}(T)$ and $R_{\text{eff}}(\text{IWC},T)$ used throughout the paper only refer to these specific parameterizations. There are many more similar parameterizations available in the literature [e.g., *Donovan*, 2003; *McFarquhar*, 2001; *McFarquhar and Heymsfield*, 1997; *Ebert and Curry*, 1992] which will probably give different results in the comparison presented in this work, and they should be compared in a similar manner in future studies. The third parameterization uses a constant value of 30 μm for all ice clouds.

[12] Finally, a new R_{eff} parameterization based on geometrical cloud thickness is used, hereafter referred to as $R_{\text{eff}}(H,Z)$, where H and Z, respectively, denote the total geometrical cloud thickness and the depth into cloud from cloud top [*van Zadelhoff et al.*, 2004; G.-J. van Zadelhoff et al., An effective radius parameterization for ice clouds using cloud thickness, submitted to *Geophysical Research Letters*, 2007]. This parameterization is based on observations made at the Atmospheric Radiation Measurement Program Southern Great Plains (ARM-SGP) site (longitude, 97.49°W; latitude, 36.61°N; United States of America) and at the Cabauw Experimental Site for Atmospheric Research (longitude, 4.93°E; latitude, 51.97°N) in the Netherlands. The functional form is a parabola, with coefficients depending on the total cloud thickness. The cloud-depth relationship applied in this parameterization is the same for both sites, in contrast to the temperature- and IWC-based parameterizations, even though the two sites are located in entirely different climate regimes. It is therefore assumed that the relationship is applicable to all ice clouds, at least in the midlatitude, but not to anvils associated to deep convective systems (the enhanced vertical mixing within these clouds lead to larger ice crystals). Future observations from CloudSAT [*Stephens et al.*, 2002] and CALIPSO [*Winker et al.*, 2003] should verify whether this assumption is valid or not. The cloud-thickness relationship is inferred from observations of ice-clouds with an optical thickness smaller than ~4, i.e., those clouds that could be fully probed from bottom to top by the lidar and the radar. The relationship might therefore not be applicable to optically thicker clouds. It is, however, assumed in this work that it holds for all ice-clouds.

[13] In order to assess how the different parameterizations affect the shortwave radiative transfer the response of a stand-alone radiation code (from RACMO2) to a prescribed atmospheric forcing has been investigated. The results are discussed in the next section.

3. Radiation Effects for a Single Column

[14] In the previous section the different parameterizations have been introduced. In order to evaluate the effects of the parameterization on the shortwave radiation and to quantify the differences between calculated and observed irradiances, the parameterization has been included in the stand-alone version of the ECMWF radiation module (cy23r4). This is also the standard radiation module used in the current RACMO2 release.

[15] In order to compare the calculated to the observed fluxes, the atmospheric column has to be as close as possible to the observed vertical structure of the atmosphere. In addition to the general parameters like temperature, pressure, and humidity, this includes the cloud properties IWC, cloud cover, and R_{eff}. The general parameters are taken from the ECMWF-IFS analysis for the column above Cabauw, and the aerosol amounts are adopted from a standard aerosol climatology following the work of *Tanre et al.* [1984]. IWC and cloud cover are retrieved from the KNMI cloud radar reflectivity, and the R_{eff} is considered the free parameter for which the SW fluxes are compared. The KNMI 35-GHz cloud radar at Cabauw has been operated virtually nonstop from 2001 up to the first half of 2005 and from November 2005 onwards, giving a nearly continuous database with a 15.5-sec temporal resolution and 90-m vertical resolution up to 11.5 km. Since Cabauw was part of the EU-funded CloudNET program, the entire database can be found at www.cloud-net.org. The radar reflectivity is proportional to the square of the particle mass, which makes the cloud radar extremely useful for detecting the large particles in ice clouds. In general, the cloud radar misses clouds above 12 km and the (high cirrus) clouds with very small particles. Such clouds can, however, be detected by a lidar if the total optical thickness below these clouds is sufficiently small. From the database a sample of 13 days (dates used in this paper: 18 June 2003, 16 August 2003, 15 September 2003, 26 November 2003, 21 February 2004, 4 April 2004, 25 April 2004, 26 August 2004, 17 September 2004, 5 November 2004, 2 December 2004, 4 March 2005, 20 March 2005, for details and data see www.cloud-net.org) has been selected, each with persistent ice cloud coverage for at least a few hours. The days were chosen to have no liquid clouds present. It is assumed that the amount of persistence inferred from the observed time series is representative for the entire cloud-field, also in the perpendicular direction, giving the one-dimensional column (plane-parallel) calculations a reasonable resemblance of the true three-dimensional radiative transfer through the cloud-field. In Figure 1 an example of the measured radar reflectivity during one of these days (25 April 2004) is shown.

[16] From the radar reflectivity and temperature profiles, the IWC is retrieved applying an empirical retrieval proposed by *Hogan et al.* [2006]. This retrieval has been derived using in situ measurements and should provide a good representation of the local IWC. After mapping the observed cloud properties on the model vertical mesh the atmospheric profiles are fed into the stand-alone radiation code.

[17] An example of such an atmospheric profile as derived for 11:43 UTC on 25 April 2004 is shown in Figure 2,

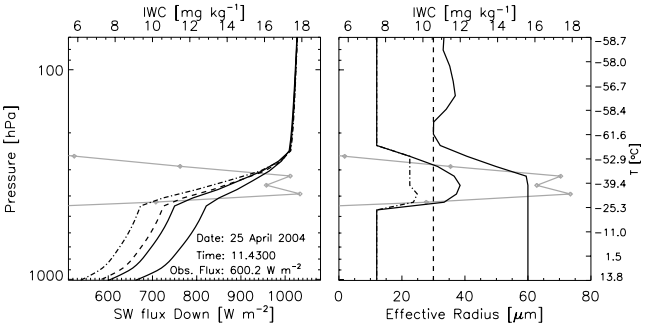

Figure 2. Atmospheric profile at 11:43 UTC on 25 April 2004 showing the calculated shortwave flux profiles in the left panel and the effective radius according to each of the four parameterizations in the right panel. The global radiation measured at this instant was 600.1 W m^{-2}. The solid line shows the currently used T-based parameterization (see Figure 6b). The dashed line shows the constant R_{eff} of 30 μm, the dashed-dotted line is based on T and IWC, and the dashed-triple dotted line is the R_{eff} parameterization. The grey line shows the IWC retrieved for this cloud, with the diamonds showing the individual cloud pixels.

given are vertical profiles of the calculated shortwave flux profiles for the four R_{eff} parameterizations, the IWC profile, and the R_{eff} parameterizations themselves as a function of both pressure and temperature. The parabolic shape of the $R_{\text{eff}}(H,Z)$ parameterization is clearly discernible, and the cloud layer is found well represented in the model by six cells. The optical thickness and hence the downwelling shortwave flux depend on the vertically integrated IWC/R_{eff} ratio. In this example the IWC profile is fixed thereby relating the flux directly to the particle size profile. The $R_{\text{eff}}(H,Z)$ parameterization shows a lower SW flux compared with the current temperature-based parameterization because of the smaller particle sizes. The $R_{\text{eff}}(\text{IWC},T)$ on the other hand assigns too small particles resulting in a too low surface SW flux.

4. Statistical Analysis

[18] In the previous section the various R_{eff} parameterizations have been compared qualitatively by examining their performance for a single atmospheric profile. In this section the parameterizations are evaluated in a more statistical approach. The profiles derived for the 13 days, mentioned earlier, are sampled at a 30-sec temporal resolution, and only those profiles which fall within a 10-minute overcast window, without any cloud-pixels identified as liquid water, are retained for further analysis. The former requirement is to ensure that the independent column approximation (ICA) is justified, using the one-dimensional plane parallel radiative transfer assumption; the latter is to reduce external influences that are not due to ice clouds. For all remaining profiles, the calculated fluxes are compared to the measurements and normalized to the top of atmosphere (TOA) incoming flux (transmissivity). The transmissivity is used to exclude effects related to, for example, differences in solar zenith angle. Distributions of the differences in transmissivity for the different parameterizations are shown in Figure 3.

[19] In the Tables 1 and 2 the differences in the SW radiative flux and transmissivity are summarized, respectively. The first two columns of Table 2 contain the parameters that describe the distributions seen in Figure 3. The distributions appear to be non-Gaussian, as indicated by their long tails and by the positive skewness of 0.20, leading to differences between the mean and median flux between 5 and 11 W m^{-2} for the different parameterizations. The median, unlike the mean, represents the most probable value for skewed distributions. The results are therefore discussed in terms of the median of the distributions. In Table 1, the 33-, 50-, and 67-quantile values of the distributions are listed together with the error in the median value. The 33- and 67-quantile values give a hint of the width of the distribution. The error in the median is calculated using bootstrapping. This method uses the actual data

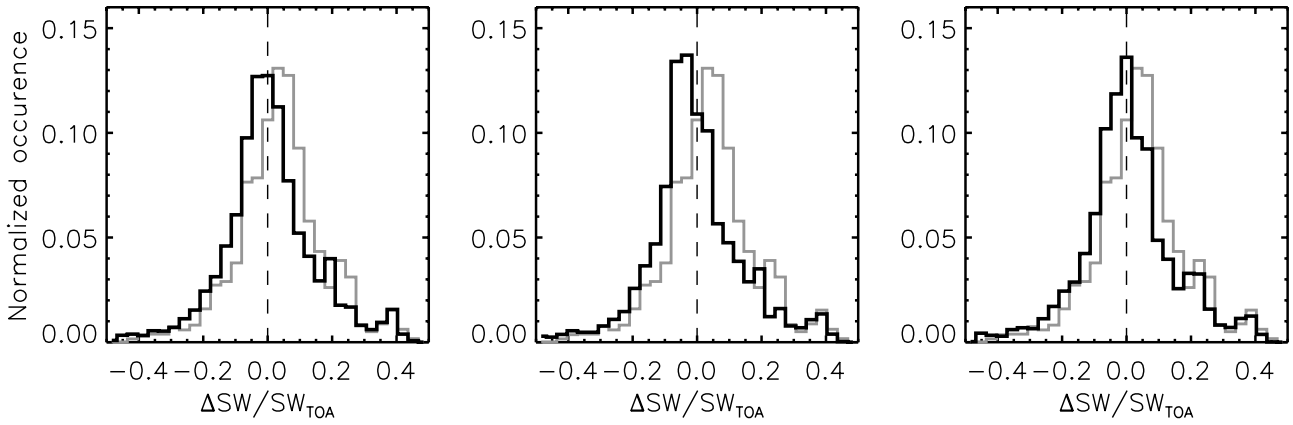

Figure 3. Distributions of the normalized differences between the calculated and measured shortwave fluxes for the different parameterizations. The grey distribution seen in the three panels represent the current temperature-based distribution. In Figure 3a the black line represents the distribution for particles with a constant 30-μm size, in Figure 3b the line shows the IWC and T-based parameterization, and Figure 3c shows the distribution using the $R_{\text{eff}}(H,Z)$ parameterization.

Table 1. Parameters Describing the Distributions of the Differences in Calculated Versus Measured Fluxes [W m^{-2}][a]

Model	Median	δ-Median	33%	67%
$R_{eff}(T)$	15.3	0.5	2.8	35.5
$R_{eff}(30\ \mu m)$	−1.5	0.7	−17.4	10.7
$R_{eff}(IWC,T)$	−7.0	0.6	−26.0	5.1
$R_{eff}(H,Z)$	0.7	0.6	−15.9	12.8

[a]The columns list the median, the error in the median, and the 33- and 67-quantiles of the distributions.

set to construct synthetic data sets by randomly drawing values from the original set (e.g., *Press et al.* [1992] and *Efron and Tibshiran* [1993] for more information). The standard deviation of the retrieved median values is assumed to be the error in the median.

[20] The $R_{eff}(H,Z)$ parameterization shows a smaller median difference in both transmissivity (0.2%) and SW flux at the surface (0.7 W m^{-2}) than the three other parameterizations, although the constant 30-μm parameterization results in similarly small differences, −0.4% and −1.5 W m^{-2}, respectively. The current RACMO2 parameterization overestimates the median shortwave flux by about 15 W m^{-2} and the transmissivity by 4% due to the assumption of too large particles within ice clouds. The $R_{eff}(IWC,T)$ parameterization underestimates the median of the SW flux by about 7 W m^{-2} (transmissivity by −1.9%) indicating that the particles are too small.

[21] As discussed before, the $R_{eff}(H,Z)$ parameterization is formulated using the total geometrical thickness of the clouds. This was originally derived for optically thin cases only ($\tau < 4$), and it is therefore of importance to check whether the parameterization holds for the clouds used in this comparison. In Figure 4, such a check is presented where the differences in SW flux are subdivided into different geometrical cloud-thickness bins with a resolution of 0.75 km. For each bin the median value of the resulting distributions is calculated and plotted for each of the R_{eff} parameterizations. Linear fits are included to guide the eye. The fits are based on the results for all cloud thicknesses with the exception of the 3.75–4.5 km bin because it was found that the median values of this thickness range show a comparable shift to too positive values for all parameterizations. This indicates that part of the cloud sample that was found to have a thickness within this bin might not have been probed in its full vertical extension, so that either the top part of these clouds are not observed or an entire cloud at higher altitudes is missed by the radar.

[22] The values in Figure 4 indicate that the $R_{eff}(H,Z)$ parameterization provides a fairly accurate median for all cloud thicknesses. The $R_{eff}(H,Z)$ parameterization has too large particles (too small optical thickness) for each of the heights resulting in a positive difference for all bins. The good overall comparison found for the $R_{eff}(30\ \mu m)$ parameterization discussed in the previous paragraph is a result of compensating errors, since the $R_{eff}(30\ \mu m)$ parameterization assumes too large particles in thin clouds and too small particles in thick clouds. Finally, the $R_{eff}(IWC,T)$ shows a good agreement for thin clouds but underestimates the R_{eff} for thick clouds, resulting in a too large total optical thickness for these clouds. It is mentioned that these results should not be overinterpreted for clouds thicker than 4.5 km as this part of the figure is made up of relatively few points (Figure 4; right panel).

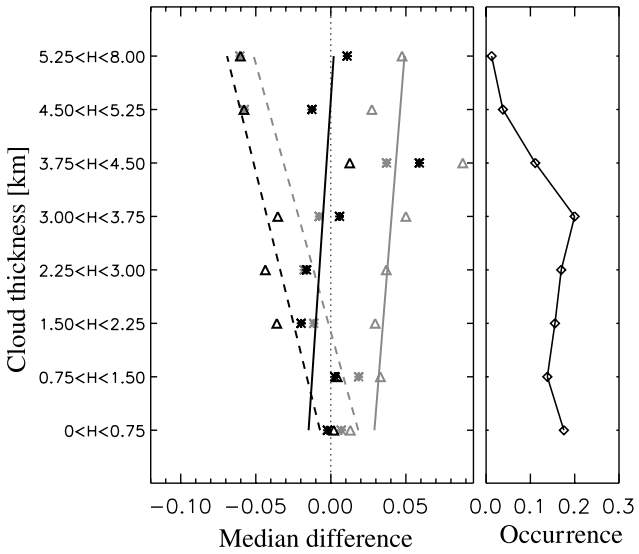

Figure 4. Medians of the difference in transmissivity presented in Figure 3 subdivided in different cloud thickness regimes (left panel). The symbols represent the following R_{eff} parameterizations: black asterisk, $R_{eff}(H,Z)$; grey asterisk, $R_{eff}(30\ \mu m)$; black triangle, $R_{eff}(IWC,T)$; grey triangle, $R_{eff}(T)$. The lines through the median points, to guide the eye, are obtained from linear fits, but with the results from the 3.75–4.5 km bin omitted. Right panel shows the fraction of the points within each of the thickness bins used. The linear fits are weighted using these values.

[23] As column or cloud structure slightly vary only between consecutive profiles, the data are correlated even though no information is transferred between different profiles. This correlation could disturb the statistics discussed before. The data set was checked in this respect, and the correlation of ice cloud properties appears to be decorrelated within half an hour. To check if any correlation contributes to a bias, the data are resampled using the bootstrap technique. The days are divided in 30-minute bins. The median in each bin is calculated and combined in an uncor-

Table 2. Parameters Describing the Distributions Presented in Figure 3[a]

	All		$\frac{1}{2}$hr-bins	
	Median	δ-Median	Median	δ-Median
$R_{eff}(T)$	4.0×10^{-2}	1.2×10^{-3}	4.5×10^{-2}	8.2×10^{-3}
$R_{eff}(30\ \mu m)$	-4.1×10^{-3}	1.5×10^{-3}	-3.5×10^{-3}	8.7×10^{-3}
$R_{eff}(IWC,T)$	-1.9×10^{-2}	1.5×10^{-3}	-1.2×10^{-2}	8.6×10^{-3}
$R_{eff}(H,Z)$	2.0×10^{-3}	1.3×10^{-3}	1.9×10^{-3}	8.7×10^{-3}

[a]Listed are the median transmissivity and standard deviation using all available points and only half-hour values, respectively. The half-hour values are calculated as indicated in the text.

related data set. The results are presented in Table 2. The median values hardly change for the half-hour bins. The error estimate in the median is enhanced because of the lower amount of points within the statistics compared with the 30-sec resolution data.

[24] The differences between the observed and calculated median and the large spread observed for each of the distributions shown in Figure 3 can be explained as follows. The $R_{\mathrm{eff}}(H,Z)$ parameterization assumes the complex polycrystal habit of *Mitchell et al.* [1996] and a bimodal gamma particle size distribution (PSD). This specific habit and PSD were adopted as they gave the best fit to the remote sensing data at the ARM-SGP site [*Donovan*, 2003]. It can be argued that, during a number of the days that were examined, the ice crystal properties in the clouds above Cabauw were not adequately represented by the assumed properties. As long as the dominant ice crystal property is well represented, different ice crystal shapes would induce a larger spread; however, when a different property represents the dominant species, the distribution could be entirely shifted. The parameterization itself is derived from an effective radius distribution with a certain spread. The application of this parameterization should lead to an underestimation of the intrinsic spread of the microphysical properties seen in ice clouds and therefore lead to a spread in the derived fluxes. The same argumentation can be given with respect to the IWC determination. The parameterization of IWC in terms of radar reflectivity and temperature [*Hogan et al.*, 2006] is based on aircraft measurements. Interpretation of aircraft measurements has its own problems as neither the entire range of particle sizes nor the IWC below a certain value (for example, 0.01 g m^{-3}) can be inferred from the raw measurements without making assumptions. This need for a proper description of the distribution and not just the median values was previously noted by *McFarquhar et al.* [2003] and *Iacobellis et al.* [2003]. Even if this is done properly, the database is still limited in time and space and might contain a bias toward the most common ice crystal properties that prevailed during the European Cloud and Radiation Experiment (EUCREX) campaign on which the IWC(Z,T) parameterization is based. The predominant ice crystal properties in the 13 days used in the present evaluation are not necessarily the same as the one during the EUCREX campaign.

[25] An important shortcoming in the calculation of the SW flux may be the plane parallel assumption. Even though days with persistent ice clouds were chosen for which the plane parallel assumption seems reasonable, there are most likely three-dimensional effects, for example, three-dimensional variations in the cloud, aerosol, and water vapor distributions which have not been accounted for. It is thought that the large standard deviation present for all the distributions is an expression of this effect.

[26] Another effect which was not included is that of missing cirrus clouds. The radar (operating at a frequency of 35 GHz) is very sensitive to the particle size/mass and has problems with detecting small ice crystals ($<10-20$ μm depending on IWC and distance to the radar). Also, ice clouds above 12 km will be missed and can therefore not be taken into account. The effect of including the undetected clouds would be an increase of optical thickness and an even lower calculated flux making the differences for all parameterizations, with the exception of the $R_{\mathrm{eff}}(T)$ parameterization, even larger.

[27] Finally, the statistics could be influenced by the small number of days for which good persistent ice cloud decks are found. It is possible that the distribution is shifted slightly owing to a single day that is affected by a large number of correlated offsets.

5. Implementation of the New Parameterization in a Climate Model

[28] Having assessed and evaluated the direct influence of the R_{eff} parameterization on the SW radiative transfer with observations of shortwave radiation fluxes at the surface, the impact of the different parameterizations on the performance of the KNMI regional climate model (RACMO2) will be investigated. Before presenting the results, the implementation of the $R_{\mathrm{eff}}(H,Z)$ parameterization in RACMO2 is discussed. The model employs hybrid vertical coordinates with a fixed number of layers. Ice clouds are described by their cloud fraction, ice water content, and effective radius. Cloud condensate and cloud fraction are prognostic variables, whereas the ice/water fraction is diagnosed on the basis of temperature. In all four parameterizations discussed in this paper, R_{eff} is diagnosed from local properties (for example, temperature, IWC); however, the $R_{\mathrm{eff}}(H,Z)$ parameterization also contains nonlocal terms as it depends on the cloud vertical extent.

[29] In order to compute these nonlocal terms, the $R_{\mathrm{eff}}(H,Z)$ parameterization, which is based on geometrical thickness, must be linked with the model vertical mesh. The vertical resolution in the model ranges from 0.3 to 0.8 km for altitudes of 3 to 12 km.

[30] In the following description, cloud fraction (c_{f}^{i}) is used for the fraction of the total area covered by clouds within a single model layer i and total cloud cover for the total area covered by all clouds in the column. The c_{f}^{i} is decomposed into different cloud fractions ($c_{\mathrm{f}}^{i}(k)$), where k denotes the components of the decomposition. The decomposition depends on the cloud fraction overlap between adjacent layers. It is assumed that, within a model layer, there is no subgrid scale distribution in the vertical. If two or more adjacent layers have a nonzero cloud fraction and IWC, a part of the cloud will have a thickness equal to the total thickness of these layers. This part of the cloud is defined by $c_{\mathrm{f}}^{i}(k = 1)$ which is equal to the minimum horizontally overlapping cloud fraction in adjacent layers, assuming maximum overlap. The layers are subsequently checked for the next minimum in the c_{f}^{i} profile. The procedure of checking adjacent cloud layers for overlapping cloud fractions is repeated until the entire c_{f}^{i} has been decomposed.

[31] A sketch displaying how this works out for a region of seven adjacent model layers with a cloud fraction greater than 0 and a total cloud cover of 0.4 is shown in Figure 5. In this example the cloud fraction profile can be decomposed into three contributions. The first contribution has a thickness equal to all seven layers ($c_{\mathrm{f}}^{i}(k) = 0.1$). The second contribution defines two separate clouds with a total thickness of three layers ($c_{\mathrm{f}}^{i}(k) = 0.2$ and 0.1), and the third contribution shows two separate clouds (one and two layers thick; $c_{\mathrm{f}}^{i}(k) = 0.1$). For each of the thicknesses the $R_{\mathrm{eff}}(H,Z)$

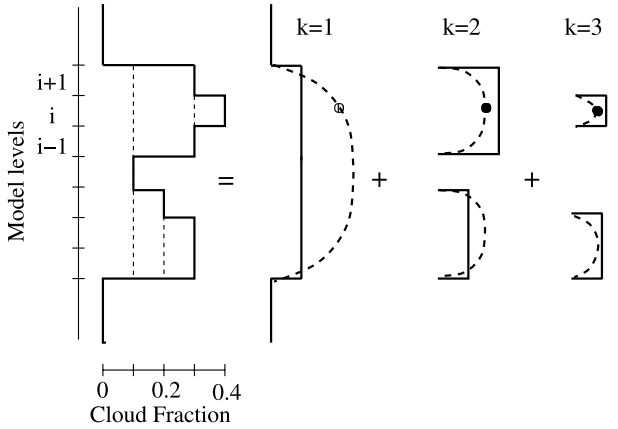

Figure 5. Sketch of the R_{eff} assignment to different cells using the cloud fraction profile as the input. From left to right the figure shows the cloud fraction profile and its decomposition into three contributions. The parabola shows the R_{eff} parameterizations for each of the total cloud thicknesses, and the dots show the values of $R_{\text{eff}}(i,k)$ which need to be combined to calculate the effective R_{eff} for model layer i.

parameterization calculates the local effective radius ($R_{\text{eff}}(i,k)$). For a model layer containing multiple contributions, the grid cell effective R_{eff} has to be calculated. Since the R_{eff} is required for the radiative transfer calculation, the effective is R_{eff} computed as the $c_{\text{f}}^{i}(k)$ reciprocal of R_{eff} (cloud optical thickness $\propto R_{\text{eff}}^{-1}$).

$$R_{\text{eff}}^{-1}(i) = \frac{1}{c_{\text{f}}^{i}} \sum_{k=0}^{k=K} \frac{c_{\text{f}}^{i}(k)}{R_{\text{eff}}(i,k)} \tag{1}$$

[32] The calculation of the effective R_{eff} will no longer be needed after the Monte Carlo Independent Column Approximation (McICA [*Barker et al.*, 2002]) has become part of the radiative transfer code. A scheme like McICA automatically takes care of subgrid variations and is, in fact, ideally suited for this type of problem.

[33] As the first test of the implementation of the $R_{\text{eff}}(H,Z)$ parameterization the resulting temperature relationship has been checked. In many of the R_{eff} parameterizations applied in present-day climate models, temperature plays an important role. The $R_{\text{eff}}(H,Z)$ parameterization does not utilize temperature as a direct input parameter. It is of interest to see if any of the adopted parameterizations is capable of returning a temperature distribution ($R_{\text{eff}}(T)$) comparable with the observed distribution. The retrieved distribution (Figure 6a) is based on observations made at the Cabauw site, and it shows the ice clouds that were observed using the combined radar and lidar technique between October 2001 and June 2003. All clouds have been included, also the ones which were not fully penetrated by the lidar. Consequently, an extra peak emerges at high temperatures ($-10°$–$0°$C) compared to the $R_{\text{eff}}(T)$ distribution from which the parameterization was derived [*van Zadelhoff et al.*, 2004]. It was chosen to retain these points in the comparison as these clouds are represented by the model.

[34] The comparison between the observed and modeled $R_{\text{eff}}(T)$ distributions is performed by operating the ECMWF stand-alone radiation scheme for three of the R_{eff} parameterizations ($R_{\text{eff}}(T)$, $R_{\text{eff}}(H,Z)$, $R_{\text{eff}}(\text{IWC},T)$) forced by atmospheric profiles obtained from a single RACMO2 forecast run for 1 month (May 2003). For each day, only the 12:00 UTC state is considered and checked for clouds for which the total water content consist of at least 80% ice. The values of R_{eff} and the temperature for these cells are combined, resulting in a distribution for each of the parameterizations. Figure 6 shows the results together with the retrieved values at Cabauw. In Figure 6b the $R_{\text{eff}}(T)$ parameterization is shown. This parameterization returns larger particle sizes compared to the observed mean and, by the nature of the parameterization, the distribution can be described by a linear relationship with a minimum and maximum value. Figure 6c shows the parameterization based on cloud thickness, resulting in a distribution which reasonably well resembles the observed distribution. In the mean the observed R_{eff} is overestimated for temperatures less than $-20°$C (up to a factor of two), whereas they compare well for temperatures above $-20°$C. There are two reasons for this overestimation. First, it reflects the difference in minimum cloud thickness allowed (the vertical extent of a model layer) in the algorithm, and second, the current parameterization uses the center model layer height to calculate the R_{eff} within the parabola. In a future version this will be replaced by a modified R_{eff} that corresponds to

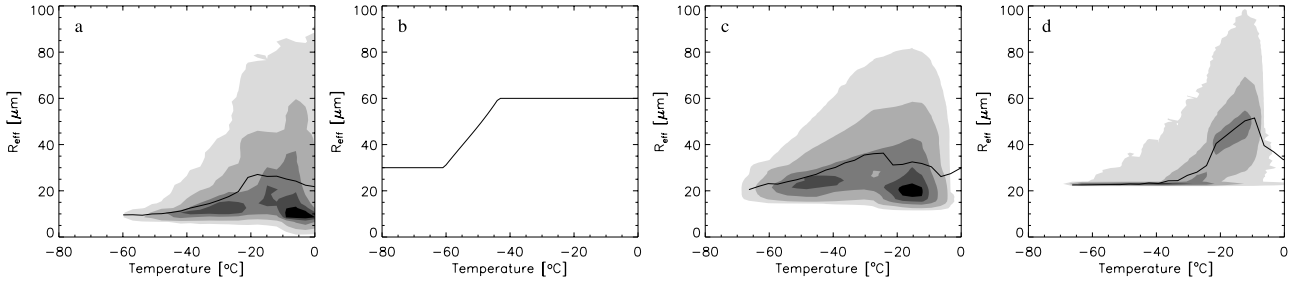

Figure 6. (a) Distributions of temperature versus effective radius for observations retrieved from Cabauw, (b) current operational parameterization used in RACMO2 and ECMWF-IFS L60, (c) new $R_{\text{eff}}(H,Z)$ experimental parameterization, and (d) particle effective radius based on T and IWC, from the work of *Sun and Rikus* [1999], which is used in the latest ECMWF-IFS runs (cy30r1). The grey-scales, from dark to light, show the 10, 30, 60, 90, and 95% probability of occurrence for all the measurements. The mean $R_{\text{eff}}(T)$ is given by the solid line.

the layer-integrated optical depth (α = IWC / ($aR_{\mathrm{eff}}(z)^2$ + $bR_{\mathrm{eff}}(z)$ + c)). The midpoint value results in an overestimation of the R_{eff} compared with the modified R_{eff}. Both effects combined result into the larger minimum R_{eff} and mean values for low temperatures as is seen in Figure 6c.

[35] The R_{eff}(IWC,T) (Figure 6d) distribution has a lower limit of 22.5 μm, which is larger than the observed minimum, resulting in a large number of values in this size bin. The mean particle size increases for temperatures above −35°C. This distribution does not show the large amount of clouds with relatively small particles at high temperature as is seen in the observations. This artificial lower limit is due to specific assumptions made in parameterization of *Sun* [2001]. The originally observed data from which this parameterization was derived has a lower limit of 15 μm and shows a spread in its distribution [*McFarquhar and Heymsfield*, 1997]. However, since clouds with optical thickness greater than four were not fully sampled in the observations, this part of the distribution lacks statistical significance.

[36] In conclusion, the distribution of the parameterization based on cloud thickness best reflects the observed $R_{\mathrm{eff}} - T$ distribution even though temperature information was neither used in deriving the parameterization from the observations nor in applying the parameterization to the radiation scheme of RACMO2. The other two parameterizations, which use temperature as a direct input parameter, perform not as well as the $R_{\mathrm{eff}}(H,Z)$ parameterization.

6. Effects on a Regional Scale

[37] In this section the impact on the shortwave radiation flux of various R_{eff} parameterizations is investigated. This is done on an extended temporal and spatial scale by performing forecast runs for an entire year (1995) in the domain in between 62°W, 62°E, 27° and 75°N. The results are presented in terms of their mean monthly values, which are calculated using the hourly values from each run.

[38] In Figure 7, the resulting mean difference between the $R_{\mathrm{eff}}(H,Z)$ and $R_{\mathrm{eff}}(T)$-based incoming shortwave radiation flux at the surface and outgoing shortwave radiation flux at the top of atmosphere (TOA) for the month of September is shown. As the $R_{\mathrm{eff}}(H,Z)$ particle sizes are nearly always smaller in comparison with the $R_{\mathrm{eff}}(T)$ parameterization (Figures 6b and 6c), the flux at the surface is lower, with a mean difference of −2.8 W m^{-2} for the entire domain for this month and a local maximum difference of −14.7 W m^{-2} over Greenland (not shown). The reflected flux at the TOA shows the reverse relationship with the incoming flux, also due to the smaller particles. The mean difference for the entire domain is +2.9 W m^{-2}. The IWC and c_{f} are very similar in both runs, with 60 and 95% of all the ice-clouds' pixels having values within 5 and 10% of each other, respectively. These differences arise, as for each day, small changes in clouds occur owing to differences in the radiative heating. However, the differences in IWC and c_{f} remain small since each member of the forecast series is initiated every day from the same prescribed atmospheric state in either of the two runs. The mean differences presented above provide lower limits since all hourly values are used (both day and night). The true difference is therefore roughly about a factor of two higher.

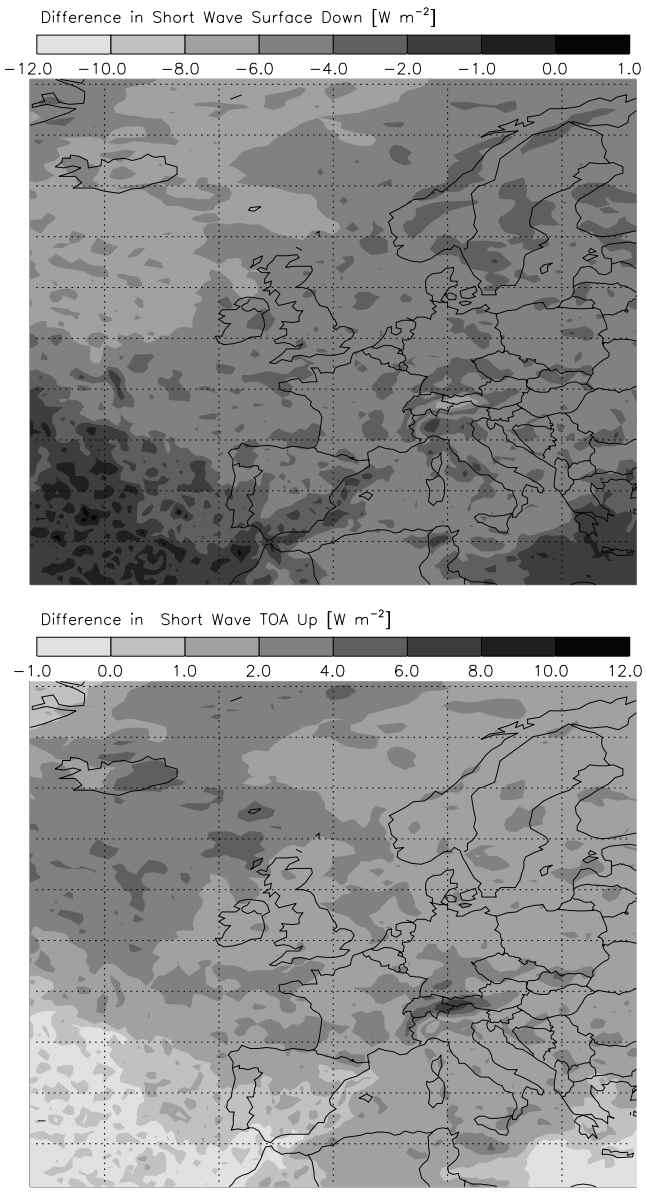

Figure 7. Difference in mean incoming shortwave flux (W m^{-2}) at the surface (top panel) and mean reflected shortwave flux at the top of atmosphere (W m^{-2}) obtained from RACMO2 hindcast runs for the month September 1995. Compared are the $R_{\mathrm{eff}}(H,Z)$ ice size parameterization to the current ($R_{\mathrm{eff}}(T)$) parameterization.

[39] Note that throughout the domain the surface fluxes are lower and the TOA fluxes are higher for the $R_{\mathrm{eff}}(H,Z)$ parameterization, except for a few single cells above the Atlantic Ocean (off the coast of Portugal), where the surface flux differences are slightly positive.

[40] Comparing the fluxes and their means directly can be misleading for the winter months as the northern part of the domain hardly receives any solar radiation, resulting in only small differences in the absolute fluxes at the surface. To compensate for this, the difference in flux is normalized with the top of the atmosphere incoming flux, resulting in the difference in transmissivity and planetary albedo. In Figure 8, the difference in transmissivity between $R_{\mathrm{eff}}(H,Z)$

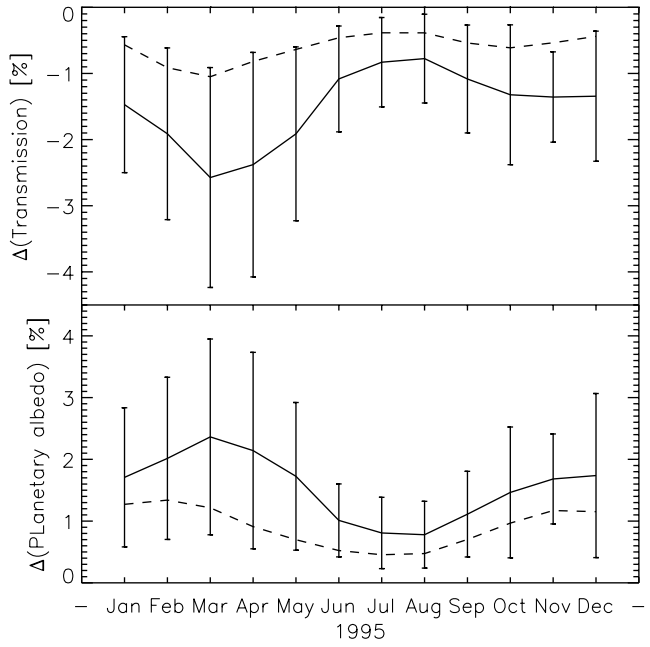

Figure 8. Mean difference in the transmissivity (%) (top panel) and planetary albedo (%) (bottom panel) for each month in 1995. The solid line denotes the difference between the $R_{\text{eff}}(H,Z)$ and $R_{\text{eff}}(T)$ parameterizations, and the dashed line denotes the difference between the $R_{\text{eff}}(\text{IWC},T)$ and $R_{\text{eff}}(T)$ parameterization. The error bars denote the standard deviation derived for the entire domain shown in Figure 7.

and the $R_{\text{eff}}(T)$ parameterization is plotted for 1 year (1995) of model results, showing differences up to 2.6% for the entire grid. The minimum in the spring of 1995 is due to large prevailing cloud-fields in the northern part of the Atlantic Ocean for this period. Also shown is the difference between the $R_{\text{eff}}(\text{IWC},T)$ and $R_{\text{eff}}(T)$ parameterizations, averaged over the entire domain, which shows a difference of up to -1.1%.

[41] Differences in planetary albedo for $R_{\text{eff}}(H,Z)$ and $R_{\text{eff}}(\text{IWC},T)$ compared with the $R_{\text{eff}}(T)$ are found to be in the order of 2.4 and 1.3%, respectively. The effects found in this section are relatively small compared with what the effects would look like for a climate run. In a climate run, differences in R_{eff} on the radiation flux profiles would impose a long-term feedback on the model dynamics. For the forecast runs presented here, this effect is absent as the model is reset once a day. The flux differences have a prevailing sign whenever an ice cloud is available thereby forcing the energy balance in the same direction continuously, which would in the long term lead to different climatic solutions. A regional climate model like RACMO2 will only be kept within bounds because of the lateral forcing exerted from a single representation of the global model in which the RCM is embedded.

[42] In conclusion, the $R_{\text{eff}}(H,Z)$ parameterization has a definite effect on the energy balance relative to the temperature-based formulation $R_{\text{eff}}(T)$, which is currently used in RACMO2. The $R_{\text{eff}}(\text{IWC},T)$ parameterization, used in the latest release of the ECMWF-IFS (cy30r1), shows a smaller but still significant difference compared with the $R_{\text{eff}}(T)$ parameterization. To quantify this effect on the shortwave flux in such a way that one can decide which parameterization is more suitable for use in a regional climate model is problematic because of the lack of knowledge about the 'truth' and all the interactions and feedback mechanisms present in a (regional) climate model. A more general issue would be that the present-day climate models are balanced in such a way that the best results or skill score is achieved with the standard setup. Changing one parameterization (R_{eff}) requires a rebalancing of other parameters like IWC.

7. Conclusions

[43] In this work the effects of different R_{eff} parameterizations of ice crystals on shortwave radiative transfer have been intercompared and, whenever feasible, compared to observations. This has been performed in two ways. First, the entire problem is reduced to one of a single column over the Cabauw site in the Netherlands. The atmospheric column above the site is described as comprehensively as possible using active remote-sensing observations. The surface SW flux are computed assuming the different R_{eff} parameterizations and compared with actual surface flux measurements. This procedure is done for 13 days throughout the seasons for which persistent ice clouds were observed without liquid clouds underneath. Second, a new R_{eff} parameterization based on cloud thickness and depth into the cloud has been compared with a temperature based one, running a forecast run for an entire year using the KNMI regional climate model RACMO2.

[44] The most important conclusions can be summarized as follows:

[45] • The default ECMWF $R_{\text{eff}}(T)$ parameterization (based on the work of *Ou and Liou* [1995]) is showing the largest offset in transmissivity(+4%) compared with the observed values for the 13 days for the single column calculations. The other three parameterizations result in a better agreement where the smallest differences are given by the new $R_{\text{eff}}(H,Z)$ and $R_{\text{eff}}(30\ \mu\text{m})$ formulations.

[46] • The $R_{\text{eff}}(30\ \mu\text{m})$ performs well in the comparison as it compensates the too large fluxes for thin clouds with too small fluxes for thick clouds. The $R_{\text{eff}}(H,Z)$ parameterization appears to perform reasonably well for all the cloud thicknesses considered in this study, whereas the *used* $R_{\text{eff}}(\text{IWC},T)$ performs well for geometrically thin clouds but gives too small particles for thicker clouds.

[47] • The $R_{\text{eff}} - T$ distribution of the parameterization based on cloud thickness best reflects the observed distribution even though temperature information was neither used in deriving the parameterization from the observations nor in applying the parameterization in RACMO2. This in contrast to the other two parameterizations which use temperature as a direct input parameter.

[48] • A definite effect in the radiation balance is found (up to 2.6% in transmissivity and up to 2.4% in planetary albedo) when comparing the $R_{\text{eff}}(H,Z)$ parameterization with the current temperature based one. The $R_{\text{eff}}(\text{IWC},T)$ parameterization of *Sun and Rikus* [1999] and *Sun* [2001] shows a smaller but still significant difference to the default $R_{\text{eff}}(T)$ parameterization.

[49] ● Combining the results of the column calculations and the $R_{\text{eff}} - T$ distributions generated within RACMO2, the $R_{\text{eff}}(H,Z)$ and $R_{\text{eff}}(\text{IWC},T)$ parameterizations are found to perform best overall with the $R_{\text{eff}}(H,Z)$ giving slightly better results in both cases. The good agreement for $R_{\text{eff}}(30\ \mu\text{m})$ is partly due to cancellation of errors for different cloud-thicknesses.

[50] The distributions in shortwave radiation flux response from all R_{eff} formulations show large spreads, which makes it difficult to identify a single best parameterization. This is related to both difficulties in describing the atmospheric profile correctly and in computing the shortwave fluxes at the ground (for example, three-dimensional effects). In principle, all four parameterizations are capable of accurately predicting the median flux at the surface (for a single site) by altering their parameters. For example, changing to a slightly different constant value or shifting the $R_{\text{eff}}(T)$ parameterization to smaller particles would induce this effect. Using a different $R_{\text{eff}}(T)$ or $R_{\text{eff}}(\text{IWC},T)$ from the literature might give a better agreement than the ones presented here. However, as was noted by *van Zadelhoff et al.* [2004], a single $R_{\text{eff}}(T)$ or $R_{\text{eff}}(\text{IWC},T)$ parameterizations will not be capable of simulating or retrieving the observed median R_{eff} at different sites. Parameterization like $R_{\text{eff}}(T)$ or $R_{\text{eff}}(\text{IWC},T)$ needs local values based on the local statistical conditions, making them unsuitable to use in regional of global models. Moreover, the R_{eff} versus temperature distribution generated in the models will not represent the observed one but may only match the observed median/mean values.

[51] The plane-parallel radiative transfer is calculated using a single-column model, whereas the entire three-dimensional cloud structure contributes to the observations. The scatter could be reduced by describing the atmosphere more accurately, by calculating the IWC and R_{eff} using lidar and radar measurements, by describing the actual optical properties of the aerosols, and by using all the available data to describe the three-dimensional cloud structure. However, this goes beyond the scope of this present study, which attempts to assess the effect of different parameterizations of the effective radius on shortwave fluxes simulated by a regional climate model.

[52] Although the number of dates considered is rather limited, we may speculate that our results are representative for (low convective) ice clouds in general. It is nevertheless desirable to extend this analysis with more observations from sites like the CloudNET sites, Lindenberg, and the different ARM sites. A second issue that may be addressed in future work is how the IWC is represented in climate models as both parameters (R_{eff} and IWC) are directly linked inside the model.

[53] **Acknowledgments.** We acknowledge the Cloudnet project (European Union contract EVK2-2000-00611) for providing the Instrument Synergy/Target Categorization data, which was produced by the University of Reading and ECMWF Integrated Forecast System (IFS) using measurements from the CABAUW site. This research was funded through the SRON Program Bureau External Research (EO-052 and EO-083). The first author would like to thank Alexander Los and Nick Schutgens for useful discussions on radiative transfer and statistics.

References

Bailey, M., and J. Hallett (2000), Growth rates and habits of ice crystals between −20° and −70°C, *J. Atmos. Sci.*, *61*(5), 514–544, doi:10.1175/1520-0469(2004)061.

Barker, H. W., R. Pincus, and J.-J. Morcrette (2002), The Monte Carlo Independent Column Approximation: Application within large-scale models, in *Proceedings of the GCSS Workshop, 20-May 2002*, Kananaskis, Alberta, Canada.

de Bruyn, E. I. F., and E. van Meijgaard (2005), Verification of HIRLAM with ECMWF physics compared with HIRLAM reference versions, *Tech. rep.*, HIRLAM, Available from SMHI, S-601 76, Norrköping, Sweden.

Donovan, D. P. (2003), Ice-cloud effective particle size parameterization based on combined lidar, radar reflectivity, and mean Doppler velocity measurements, *J. Geophys. Res.*, *108*(D18), 4573, doi:10.1029/2003JD003469.

Ebert, E., and J. Curry (1992), A parameterization of ice cloud optical properties for climate models, *J. Geophys. Res.*, *97*, 3831–3836.

Efron, B., and R. Tibshiran (1993), *An Introduction to the Bootstrap*, CRC Press, Boca Raton, Fla.

Fouquart, Y., and B. Bonnel (1980), Computations of solar heating of the Earth(tm)s atmosphere: A new parameterization, *Beitr. Phys. Atmos.*, *53*, 35–62.

Francis, P. N., A. Jones, R. W. Saunders, K. P. Shine, A. Slingo, and Z. Sun (1994), An observational and theoretical study of the radiative properties of cirrus: Some results from ICE'89, *Q. J. R. Meteorol. Soc.*, *120*, 809–848.

Hogan, R. J., M. P. Mittermaier, and A. J. Illingworth (2006), The retrieval of ice water content from radar reflectivity factor and temperature and its use in the evaluation of a mesoscale model, *J. Appl. Meteorol.*, *45*, 301–317, doi:10.1175/JAM2340.1.

Iacobellis, S. F., G. M. McFarquhar, D. L. Mitchell, and R. C. J. Somerville (2003), On the sensitivity of radiative fluxes to parameterized cloud microphysics, *J. Clim*, *16*, 2979–2996.

Lenderink, G., B. van den Hurk, E. van Meijgaard, A. P. van Ulden, and J. Cuijpers (2003), Simulation of present-day climate in RACMO2: First results and model developments, *Tech. rep.*, KNMI, available from Postbus 201, 3730 AE, De Bilt, Netherlands.

McFarquhar, G. M. (2001), Comments on "Parameterization of effective sizes of cirrus-cloud particles and its verification against observation" by Zhian Sun and Lawrie Rikus (October B, 1999, 125, 3037–3055), *Q. J. R. Meteorol. Soc.*, *127*, 261–265.

McFarquhar, G. M., and A. J. Heymsfield (1997), Parameterization of tropical cirrus ice crystal size distributions and implications for radiative transfer: Results from CEPEX, *J. Atmos. Sci.*, *54*, 2187–2200, doi:10.1175/1520-0469(1997)054<2187:POTCIC>2.0.CO;2.

McFarquhar, G. M., and A. J. Heymsfield (1998), The definition and significance of an effective radius for ice clouds, *J. Atmos. Sci.*, *55*, 2039–2052, doi:10.1175/1520-0469(1998)055<2039:TDASOA>2.0.CO;2.

McFarquhar, G. M., S. F. Iacobellis, and R. C. J. Somerville (2003), SCM simulations of tropical ice clouds using observationally based parameterizations of microphysics, *J. Clim.*, *16*, 1643–1664.

Mitchell, D. L. (1994), A model predicting the evolution of ice particle size spectra and radiative properties of cirrus clouds: Part I. Microphysics, *J. Atmos. Sci.*, *51*, 797–816.

Mitchell, D. L., S. K. Chai, Y. Liu, A. J. Heymsfield, and Y. Dong (1996), Modeling cirrus clouds: Part I. Treatment of bimodal size spectra and case study analysis, *J. Atmos. Sci.*, *53*, 2952–2966.

Ou, S. C., and K.-N. Liou (1995), Ice microphysics and climatic temperature feedback, *Atmos. Res.*, *35*, 127–138.

Petch, J. C. (1998), Improved radiative transfer calculations from information provided by bulk microphysical schemes, *J. Atmos. Sci.*, *55*, 1846–1858.

Press, W. H., S. A. Teukolsky, W. T. Vetterling, and B. P. Flannery (1992), Numerical Recipes in FORTRAN, 2nd ed., 686–687 pp., Cambridge Univ. Press, New York.

Stephens, G. L., et al. (2002), The CloudSat mission and the A-Train, *Bull. Am. Meteorol. Soc.*, *83*, 1771–1790.

Sun, Z. (2001), Reply to comments by Greg M. McFarquhar on 'Parametrization of effective sizes of cirrus-cloud particles and its verification against observations' (October B,1999,125,3037–3055), *Q. J. R. Meteorol. Soc.*, *127*, 267–271, doi:10.1256/smsqj.57115.

Sun, Z., and L. Rikus (1999), Parametrization of effective sizes of cirrus-cloud particles and its verification against observations, *Q. J. R. Meteorol. Soc.*, *125*, 3037–3055.

Tanre, D., J.-F. Geleyn, and J. M. Slingo (1984), First results of the introduction of an advanced aerosol-radiation interaction in the ECMWF low resolution global model, in *In Aerosols and Their Climatic Effects*, edited by H. E. Gerber and A. Deepak, pp. 133–177, A. Deepak, Hampton, Va.

Undén, P. (2002), HIRLAM-5 scientific documentation, *Tech. rep.*, HIRLAM, Available from SMHI, S-601 76, Norrköping, Sweden.

van Zadelhoff, G.-J., D. P. Donovan, H. Klein Baltink, and R. Boers (2004), Comparing ice cloud microphysical properties using CloudNET and

Atmospheric Radiation Measurements Program data, *J. Geophys. Res.*, *109*, D24214, doi:10.1029/2004JD004967.

White, P. (2002), Physical processes (CY23R4). IFS documentation, *Tech. rep.*, ECMWF, http://www.ecmwf.int/research/ifsdocs.

Winker, D. M., J. Pelon, and M. P. McCormick (2003), The CALIPSO mission: Spaceborne lidar for observation of aerosols and clouds, in *Proc. of SPIE*, vol. 4893, edited by T. Itabe and Z. Liu, pp. 1–11, U.N. Singh.

R. Boers, D. P. Donovan, W. H. Knap, E. van Meijgaard, and G.-J. van Zadelhoff, Climate Research and Seismology, Royal Netherlands Meteorological Institute, P0 Box 201, Wilhelminalaan 10, De Bilt, 3730 AE, Netherlands. (zadelhof@knmi.nl)